Invited Paper

A New Microstructured DSC Photoelectrode for Potential High Power Conversion Efficiency

Qi-Feng Zhang (張琦鋒), Kwangsuk Park (朴光石) and Guo-Zhong Cao* (曹國忠)
Department of Materials Science and Engineering, University of Washington, Seattle, WA 98195-2120, USA

This paper includes an overview of general approaches and efforts to enhance the power conversion efficiency in dye-sensitized solar cells (DSC) and then the recent development of hierarchically structured photoelectrodes for DSC. Hierarchically structured photoelectrodes are made of submicron-sized aggregates of ZnO nanocrystallites. Such structured photoelectrodes retain the desired large surface area and crystal facets for dye molecule adsorption and possess the ability to scatter the visible light within the photoelectrodes, so as to enhance light adsorption and thus lead to more efficient photon capturing. In ZnO DSC, hierarchically structured photoelectrodes demonstrated over 200% enhancement in power conversion efficiency.

Keywords: Dye-sensitized solar cells; ZnO aggregates; ZnO nanocrystallites; ALD TiO_2 coating.

INTRODUCTION

The tremendous challenges faced regarding energy and natural resources are now widely recognized. Based on some recent studies,[1,2] the annual world-wide energy consumption of energy is currently estimated to be 4.1×10^{20} joules, or 13 trillion watts (13 terawatts (TW)). Among the energy supply, 35% is from oil, 23% is from coal, and 21% is from natural gas, with a total of 80% from fossil energy. Biomass contributes only 8% of the energy supply, nuclear energy 6.5%, and hydropower 2%. The world population is predicted to reach 9 billion by 2050, and with aggressive conservation and new technology development, the energy demand is predicted to double to 30 TW by 2050, and triple to 46 TW by the end of the century. At the same time, the oil production that is now the dominant energy resource is predicted to peak in 10 to 30 years. If the main energy supply is switched to coal, the United States may have enough reserve to last for another 100 years. However, this approach presents new challenges. Dealing with the carbon release from the burning the fossil fuels would require technologies to capture and store 25 billion metric tons of CO_2 produced annually.

The impact of human activities on the environment is also of great concern. Within 200 years of industrialization, the CO_2 content level has already increased from 280 ppm to 380 ppm. Industrial activities, mainly power generation from coal, has increased the total mercury flux from 1,600 tons/year in the preindustrial era to the current 5,000 tons/ year, with 3,000 tons of mercury being deposited in land, and 2,000 tons in the marine environment.[3] Both, the change in the climate and the aggressive measures to harness existing and alternative energy in developing countries has caused unprecedented problems in the preservation of the environment and natural resources. In a study by the National Research Council, an estimated 1.1 billion people are without access to safe drinking water and 2.2 billion people are without access to proper sanitation. In the year 2000 alone, 2.2 million deaths were attributed to water and hygiene-related problems. By 2050, 4 to 7 billion people will face water scarcity.[4]

With regards to energy and environmental preservation, there exists no single solution to the daunting challenges. Significant progress has been made in the development of renewable energy technologies such as solar cells, fuel cells, and bio-fuels.[5-10] Although these alternative energy sources have been marginalized in the past, it is expected that new technology could make them more practical and price competitive with fossil fuels. This would enable an eventual transition away from fossil fuels as our primary energy sources. Almost all alternative energy tech-

nologies are limited by the properties of current materials. For example, poor charge carrier mobility and narrow light absorption in current semiconductors limit the energy conversion efficiency of photovoltaic cells.[11-19] Thermoelectric (TE) materials typically possess a figure of merit less than 2.5.[20-22] Portable electronic power sources, such as batteries and fuel cells, have low energy and power densities due largely to poor charge and mass transport properties.[23,24] Fundamental advances in the synthesis, processing, and control of multiscale structure and properties of advanced materials would usher in more efficient energy conversion devices and high densities in energy/power storage.[25] Nanotechnology and nanostructured materials are expected to have a great impact on semiconductors in the energy, environmental, biomedical and health sciences.[26] When a material is reduced to the dimensions of the nanometer, its properties can be drastically different from the bulk regime. Nanomaterials and novel designs based on nanomaterials have demonstrated very promising results for energy conversion and storage.[27,28]

SOLAR CELLS AND DYE-SENSITIZED SOLAR CELLS (DSC)

Solar energy, as the primary source of energy for all living organisms on earth, is considered the ultimate solution to the energy and environmental challenge as a carbon-neutral energy source. Many photovoltaic devices that fulfill the energy conversion from sunlight to electricity have already been developed over the past five decades. However, widespread usage is still limited by two significant challenges; namely conversion efficiency and cost. One of the traditional photovoltaic devices, single crystalline silicon solar cells, were invented more than 50 years ago and currently make up 94% of market. Single crystalline silicon solar cells operate on the principle of p-n junctions formed by joining p-type and n-type semiconductors. The electrons and holes are photogenerated at the interface of p-n junctions, separated by an electrical field across the p-n junction, and collected through the external circuits. However, single crystalline silicon solar cells suffer from both high materials costs and energy-intensive production processes. Amorphous thin film silicon is a good replacement candidate because the defect energy levels can be controlled by hydrogenation and the band gap can be reduced so that the light absorption efficiency can be much higher than that of crystalline silicon. However, amorphous silicon tends not to be stable and can lose up to 50% efficiency within the first hundred hours. Bridging the gap between single crystalline silicon and amorphous silicon is the polycrystalline silicon film, for which a conversion efficiency of around 15% is obtained. Compound semiconductors such as gallium arsenide (GaAs), cadmium telluride (CdTe) and copper indium gallium selenide (CIGS) have received much attention because they present a direct energy gap, can be doped to either p-type or n-type, have band gaps matching the solar spectrum, and possess high optical absorbance. These devices have demonstrated conversion efficiencies of 16-32%. Although photovoltaic devices built on silicon or compound semiconductors have been achieving high efficiency for practical use, they still require major breakthroughs to meet the long term goal of very low cost ($0.4/kWh).[29-34]

Dye-sensitized solar cells (DSCs) based on oxide semiconductors and organic dyes have recently emerged as promising approach to efficient solar energy conversion at a low cost. The DSCs are a photo-electrochemical system which incorporates a porous-structured oxide film with adsorbed dye molecules as the photosensitized anode. A platinum-coated silicon wafer acts as the counter electrode (i.e., cathode), and a liquid electrolyte that traditionally contains I^-/I_3^- redox couples serves as a conductor to electrically connect the two electrodes.[35,38-42] Photons are captured by the dye monolayer, creating excitons that are rapidly split at the nanocrystallite surface of oxide film; electrons are injected into the oxide film and holes are released by the redox couples in the liquid electrolyte (Fig. 1a). Compared with conventional single crystal silicon-based or compound semiconductor thin film solar cells, the DSCs are thought to be advantageous as a photovoltaic device possessing both practical high efficiency and cost effectiveness. To date, the most successful DSC was based on a TiO_2 nanocrystalline film (Fig. 1b) combined with ruthenium-polypyridine complex dye as first reported by O'Regan and Grätzel in 1991.[43] A certified overall conversion efficiency of 11% was achieved on TiO_2-RuL'(NCS)$_3$ (namely "black dye") system, in which the spectral response of the complex dye was extended to the near-infrared region so as to absorb far more of the incident light.[35,36,44,45] The porous nature of nanocrystalline TiO_2 films drives their use in DSCs due to the high surface area available for dye molecule adsorption. Meanwhile, the suitable relative energy levels at the semiconductor-sensitizer interface, i.e., the po-
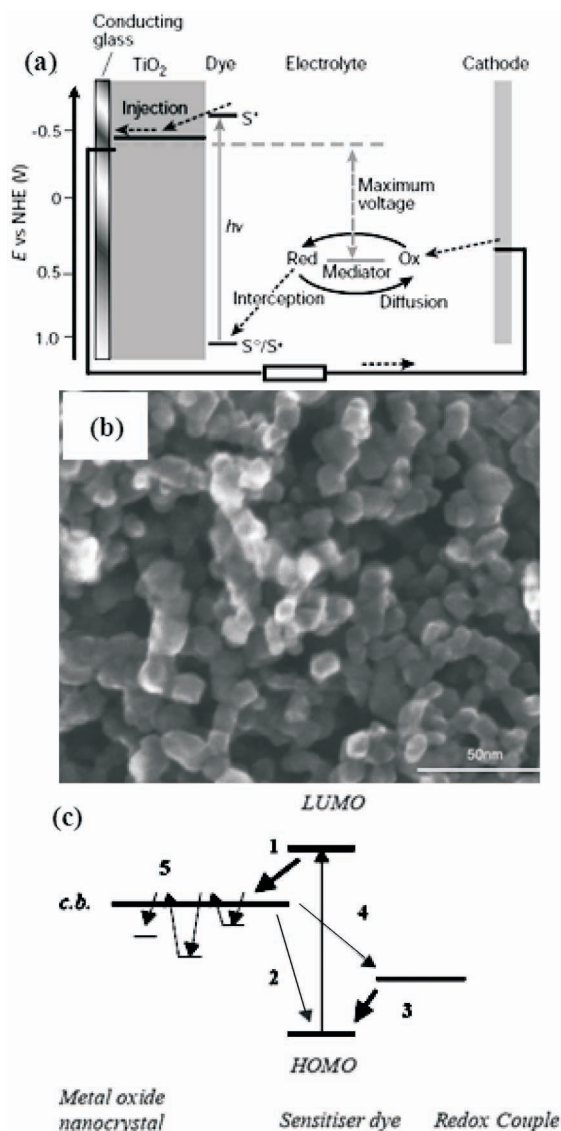
A New Microstructured DSC Photoelectrode

J. Chin. Chem. Soc., Vol. 57, No. 5B, 2010 **1121**

Fig. 1. (a) Schematic of the construction and operational principle of the device, (b) SEM image of an oxide (TiO_2) electrode film with nanocrystallites (~20 nm), and (c) Electron transport in electrodes, in which photoexcited electrons are injected from the dye to the conduction band (denoted as "c.b.") of the nanocrystallite (1), the dye is regenerated by electron transfer from a redox couple in the electrolyte (3), a recombination may take place between the injected electrons and the dye cation (2) or redox couple (4). (4) is normally believed to be the predominant loss mechanism. Electron trapping in the nanocrystallites (5) is also a mechanism that causes energy loss. LUMO and HOMO represent the lowest unoccupied molecular orbital and the highest occupied molecular orbital of the dye, respectively.[35-37]

sition of the conduction band edge of TiO_2 being lower than the excited-state energy level of the dye, allow for the effective injection of electrons from the dye molecules to the semiconductor.

The achievement of acceptable power conversion efficiencies instilled much confidence in the ability of DSCs to challenge the high costs of commercially available solar cells based on silicon or compound semiconductors. However, further increases in power conversion efficiency has been limited by the energy loss due to the recombination between electrons and either the oxidized dye molecules or electron accepting species in the electrolyte during the charge transport process.[46-48] Such a recombination originates predominately from the lack of a depletion layer on TiO_2 nanocrystallite surface. This scenario would become significantly serious when the thickness of photoelectrode film was increased.

In DSCs, the dynamic competition between the generation and recombination of photoexcited carriers has been clarified to be a bottleneck for developing higher conversion efficiency, i.e., the film thickness was desired to be larger than the light absorption length so as to capture all the photons (optically dense). Meanwhile, the film thickness was impelled to be thinner than the electron diffusion length with respect to avoiding or reducing recombination.[46,47] A variety of approaches have been explored to overcome the recombination by using either one-dimensional nanostructures that provide a direct pathway for electron transport or using core-shell structures with an oxide coating on TiO_2 to minimize the recombination rate. Aside from those approaches, a series of methods that address the generation of photoexcited carriers by combining nanostructured films with optical effects (light scattering or optical confinement)[49] has also been demonstrated to be effective in enhancing the light-harvesting capability of the photoelectrode film so as to improve the DSC performance.

Usami, Ferber, and Luther, and Rothenberger *et al.* predicted that the optical absorption of dye sensitized TiO_2 nanocrystalline films could be enhanced by admixing large sized TiO_2 particles as the light scattering centers.[50-52] The light scattering efficiency has been shown to correlate with both the size of the scattering centers and the wavelength of incident light.[53] The scattering reaches a maximum when the size of the scattering centers is about $k\lambda$, where k is a constant and λ is the wavelength. Experimentally, it has been verified that the performance of DSCs can be signifi-

cantly improved when the TiO$_2$ nanocrystalline films are combined with large-sized SiO$_2$, Al$_2$O$_3$, or TiO$_2$ particles.[54-58] By coupling a photonic crystal layer to conventional TiO$_2$ nanocrystalline films for light scattering, Nishimura *et al.* and Halaoui *et al.* also succeeded in enhancing the light-harvesting capability of the photoelectrode.[59-60] However, the introduction of large-sized particles into nanocrystalline films has the unavoidable effect of lowering the internal surface area of the photoelectrode film. This serves to counteract the enhancement effect of light scattering on the optical absorption, whereas the incorporation of a photonic crystal layer may lead to an undesirable increase in the electron diffusion length and, consequently, increase the recombination rate of photogenerated carriers. In spite of the extensive research and excellent progresses made in DSCs in the past decades, the power conversion efficiency remains relatively low when compared to single crystalline silicon solar cells.

HIERARCHICALLY SRUCTURED PHOTOELECTRODES

Our recent study has unambiguously demonstrated the fact that, compared to a nanoparticulate film, hierarchically structured ZnO photoelectrodes can significantly enhance the power conversion efficiency when all other parameters are kept constant.[61-64] Hierarchically structured ZnO films consist of submicron-sized ZnO aggregates. The synthesis of ZnO aggregates can be achieved by a hydrolysis of zinc salt in a polyol medium at 160 °C.[61] By adjusting the heating rate during synthesis and using a stock solution containing ZnO nanoparticles of 5-nm in diameter, the ZnO aggregates with an either monodisperse or polydisperse distribution in size can be prepared.[62,63] Fig. 2 shows the morphology of a hierarchically structured ZnO film and the structure of the aggregates. It can be seen that the film is well packed by ZnO aggregates with a highly disordered stacking, while the spherical aggregates are formed by the numerous interconnected nanocrystallites that have sizes ranging from several tens to several hundreds of nanometers (Fig. 2b and 2c). The structural features of the aggregates are their possession of a porosity and geometrical size comparable with the wavelengths of visible light. Four kinds of ZnO films, differing in the degree of aggregation have been prepared for a comparison of their DSC performance. Sample 1 is comprised of well-packed polydisperse ZnO aggregates, sample 2 consists of aggregates with

slight distortion of the spherical shape, sample 3 includes parts of aggregates and nanocrystallites, and sample 4 is constructed with no aggregates but dispersed nanocrystallites alone. It has been demonstrated that all these samples present approximately the same crystallite size of about 15 nm and similar specific surface area of ~ 80 m^2/g. However, their photovoltaic behaviors exhibit a significant difference in the short-circuit current density, resulting in a difference of overall conversion efficiency. Typically, a maximum short-circuit current density of 19 mA/cm^2 and conversion efficiency of 5.4% are observed for sample 1, while minimum values of 10 mA/cm^2 and 2.4% respectively are observed for sample 4. Intermediate current densities and
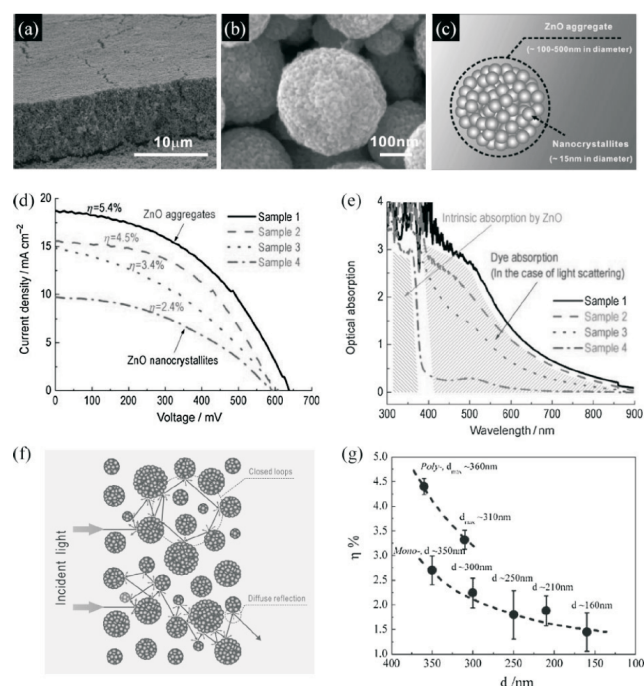

Fig. 2. ZnO aggregate dye-sensitized solar cells.[62,63] (a) Cross sectional SEM image of a ZnO aggregate film, (b) a magnified SEM image of an individual ZnO aggregate, (c) a schematic diagram illustrating the microstructure of aggregated ZnO comprised of closely packed nanocrystallites, (d) photovoltaic behaviors and (e) optical absorption spectra of N3 dye adsorbed ZnO film samples with difference in the degree of aggregation of nanocrystallites, (f) schematic of light scattering and photon localization within a film consisting of submicron-sized aggregates, and (g) dependence of overall conversion efficiency on the size and size distribution of aggregates in dye-sensitized ZnO solar cells.

efficiencies are found for samples 2 and 3 (Fig. 2d). An obvious trend is that the overall conversion efficiency becomes decreased as the degree of the spherical aggregation is gradually destructed. In other words, the aggregation of ZnO nanocrystallites is favorable for achieving a DSC with high performance.

Fig. 2e shows the optical absorption spectra of the four kinds of ZnO films previously discussed after sensitized with N3 dye. All the ZnO samples exhibit an intrinsic absorption with similar absorption intensity below 390 nm, caused by the semiconductor of ZnO with the electron transfer from valence band to conduction band. However, the absorption at wavelengths above 400 nm varies significantly, revealing the highest intensity for sample 1, a lower intensity for samples 2 and 3, and minimum in intensity for sample 4. In the spectra shown in Fig. 2e, only sample 4 presents an absorption peak centered around 520 nm. This corresponds to the visible $t_2 \rightarrow \pi^*$ metal-to-ligand charge transfer (MLCT) in N3 dye,[65] but with a slight blue-shift than adsorption of pure N3 due to the electronic coupling between N3 and ZnO. All the other samples show a monotonic increase in the absorption intensity as the wavelength varies from visible to ultraviolet. This portion of absorption is contributed by the dye molecules that are adsorbed on the ZnO surface, and the difference in the absorption intensity implies that the absorption is structure-related. It has been suggested that the difference in the absorption of samples 1-3 arises from the submicron-sized aggregates that cause the light scattering. This weakens the transmittance of films and causes a pseudo absorption in the spectra. The solar cell performance is improved due to the presence of light scattering in hierarchically structured ZnO films, by which the traveling distance of light within the photoelectrode film can be significantly extended (Fig. 2f). As such, the opportunities of incident photons being captured by the dye molecules are increased. The difference in the optical absorption of the four kinds of films implies that an improvement in the degree of aggregation of nanocrystallites would induce more effective light scattering in the visible region. A photon localization effect may also occur on these films due to their highly disordered structure that confines the light scattering in closed loops.

Further studies reinforce the light scattering mechanism. It has been demonstrated the performance of DSCs with hierarchically structured ZnO films can be significantly affected by either the average size or the size distribution of aggregates.[63] The films with polydisperse aggregates, which result in more disordered structure and achieve better packing, establish higher conversion efficiencies than those with monodisperse aggregates. The enhancement effect becomes more intensive when the maximum size of the aggregates in the polydisperse films or the average size of aggregates in monodisperse films increases to be as large as or comparable to the wavelength of visible light (Fig. 2g). These results confirm the rationality of enhanced solar cell performance arising from light scattering, generated by hierarchically structured ZnO films and promoting the light capturing ability of photoelectrode.

Compared with those large-sized TiO_2 particles or photonic crystal layer ever reported elsewhere,[55,59-60] the method using controlled ZnO aggregation of nanocrystallites in DSCs presents obvious advantages in the generation of light scattering meanwhile without causing detrimental loss in internal surface area of the photoelectrode film. That is, the size of these aggregates is on submicron scale comparable to the wavelength of visible light, so that an efficient scattering to the incident light would be established within photoelectrode film and thus extends the traveling distance of photons being absorbed by dye molecules with more opportunities. Meanwhile, the film with aggregates consisting of interconnected nano-sized crystallites provides a highly porous structure, ensuring large specific surface area for dye adsorption, unlike the large-sized TiO_2 particles with solid core that consume the internal surface area or the photonic crystal layer that is added to generate light scattering but with increased film thickness as well as electron diffusion length.

In spite the fact that ZnO has the similar electronic structure to and higher electron mobility than that of anatase TiO_2,[66] ZnO based DSC demonstrated much lower power conversion efficiency than that of TiO_2 based DSC. The relatively lower power conversion efficiency in ZnO DSC can be at least partly attributed to the relative instability of ZnO when exposed to dye solutions for the dye loading as ZnO readily reacts with dye molecules to form insulating complexes.[67-69]

One way to improve the power conversion efficiency of ZnO DSC is to modify the surface chemistry as a form of core/shell structure.[70] Atomic layer deposition (ALD) would be an ideal technique for the core/shell structure due to its unique self-limiting nature and low growth temperature, which make it possible to apply ultra-thin layer on the core,

even it is a porous structure.[71,72] ALD has been used to deposit ultra-thin TiO$_2$ layer on the porous structure of the film made of ZnO aggregates and demonstrated much enhanced PCE of ZnO DSC with photoelectrodes made of submicron-sized aggregates of ZnO nanocrystallites. As illustrated schematically in Fig. 3a, 3b, and 3c, TiO$_2$ ultra-thin layer deposited by ALD would form a complete and conformal coverage on the surface and even inside pores of ZnO that would otherwise be exposed to dye electrolyte during the dye loading. Consequently, all the dye molecules would adsorb onto the surface of TiO$_2$ coating. Such an ultra-thin and conformal ALD coating would not change the morphology the underline ZnO structures as shown in Fig. 3e and 3f. The coating of TiO$_2$ layer on the surface of ZnO by ALD is presumably so thin that would not affect any detectable change in the morphology by means of SEM. Based on the literatures, the thickness of TiO$_2$ grown by ALD for 10 cycles is estimated to be 0.3-0.6 nm.[73,74] In addition, the connections between adjacent ZnO nanocrystallites would retain to ensure a favorable electron motion through ZnO (as suggested in Fig. 3d). Such structure would improve the surface stability with enhanced dye

loading on the ZnO surface, while retain the advantage of high electron mobility in ZnO. BET results demonstrate that micropores inside each aggregate still remain after ALD, indicating the porous structure of ZnO is preserved. The preservation of the porous structure is very important to achieve the higher performance of DSCs in terms of the surface area. The slight decrease in the size and volume of the micropore was observed due to the introduction of ALD-TiO$_2$ layer. The ultra-thin ALD-TiO$_2$ layer did not cause any morphological change of ZnO aggregates, including their micropore structure. This ZnO core/TiO$_2$ shell structure is expected to suppress recombination due to the formation of n-n$^+$ heterojunction at the ZnO/TiO$_2$ interface.[75] Electrochemical impedance spectroscopy (EIS) showed the suppressed recombination at the aggregate/electrolyte interface due to the introduction of ALD-TiO$_2$ layer. It is known that the suppressed recombination also increases a fill factor (FF).[76] Therefore, the introduction of the TiO$_2$ ultra-thin layer results in more than 20% enhancement in the PCE from 5.2% to 6.3%.[77] The ALD-TiO$_2$ layer increased both the open circuit voltage and the fill factor as a result of the suppressed surface charge recombination.

CONCLUSION

There have been great efforts to advance the fundamental understanding and the materials and device technologies of DSCs. Submicron-sized aggregation of nanoparticles has been demonstrated to be an effective way to enhance the photon capturing through the internal light scattering while retain the desired high specific surface area for dye molecule adsorption. In ZnO-based DSC, the controlled aggregation of ZnO nanocrystallites resulted in > 200% PCE enhancement. ALD is introduced to coat the surface of ZnO with sub-nanometer thin TiO$_2$ layer to improve the surface chemistry so as to prevent the formation of insulating ZnO-dye complex. It is obvious that submicron-sized aggregates of TiO$_2$ nanocrystallites with desired porous structure and surface chemistry would lead to a further improvement in DSC PCE.
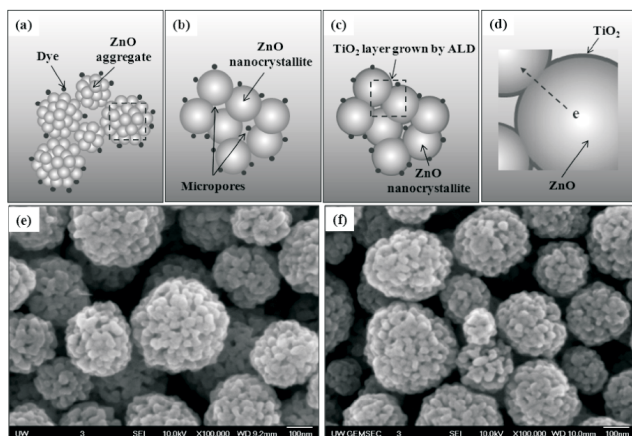

Fig. 3. Schematics illustrating (a) ZnO aggregates adsorbed with dye molecules, (b) ZnO nanocrystallites containing micropores, (c) conformal ALD-TiO$_2$ thin layer on the surface of ZnO nanocrystallites, (d) enlarged schematic showing the details of conformal ALD-TiO$_2$ coating on ZnO surface and the uninterrupted connection between adjacent ZnO nanocrystallites for efficient electron motion, and SEM images of photoelectrode films of (e) submicron-sized aggregates of ZnO nanocrystallites and (f) submicron-sized aggregates of ZnO nanocrystallites coated with thin TiO$_2$ layer.

A New Microstructured DSC Photoelectrode

J. Chin. Chem. Soc., Vol. 57, No. 5B, 2010 **1125**

REFERENCES

1. Smalley, R. E. *MRS Bulletin* **2005**, *30*, 412.
2. Office of Basic Energy Sciences, D. O. E. *Basic Energu Needs for Solar Energy Utilization; Report of the Basic Energy Sciences Workshop on Solar Energy Utilization*, 2006.
3. National Research Council. *The Environment: Challenges for the Chemical Sciences in the 21st Century*, 2003.
4. Levin, R. B.; Epstein, P. R.; Ford, T. E.; Harrington, W.; Olson, E.; Reichard, E. G. *Environ. Health Perspect.* **2002**, *110*, 43.
5. Converse, A. O. *Appl. Biochem. Biotech.* **2007**, *137*, 611.
6. Jacob, E. J. *Curr. Sci.* **2007**, *92*, 1197.
7. Shum, K. L. W. *Energy Policy* **2007**, *35*, 1186.
8. Lund, P. D. *Renewable Energy* **2007**, *32*, 442.
9. Hoffmann, W. *Sol. Ener. Mater. Sol. Cells* **2006**, *90*, 3285.
10. Gross, R.; Leach, M.; Bauen, A. *Environ. Int.* **2003**, *29*, 105.
11. Alam, M. M.; Jenekhe, S. A. *Chem. Mater.* **2004**, *16*, 4647.
12. Gregg, B. A. *J. Phys. Chem. B* **2003**, *107*, 4688.
13. Peumans, P.; Uchida, S.; Rorrest, S. R. *Nature* **2003**, *425*, 158.
14. Peumans, P.; Yakimov, A.; Forrest, S. R. *J. Appl. Phys.* **2003**, *93*, 3693.
15. Shaheen, S. E.; Radspinner, R.; Peyghambarian, N.; Jabbour, G. E. *Appl. Phys. Lett.* **2001**, *79*, 2996.
16. Dennler, G.; Sariciftci, N. S. *Proc. IEEE* **2005**, *93*, 1429.
17. Jenekhe, S. A.; Yi, S. J. *Appl. Phys. Lett.* **2000**, *77*, 2635.
18. Alam, M. M.; Jenekhe, S. A. *J. Phys. Chem. B* **2001**, *105*, 2479.
19. Xue, J.; Rand, B. P.; Uchida, S.; Forrest, S. R. *Adv. Mater.* **2005**, *17*, 66.
20. Harman, T. C.; Taylor, P. J.; Walsh, M. P.; LaForge, B. E. *Science* **2002**, *297*, 2229.
21. Venkatasubramanian, R.; Siivola, E.; Colpitts, T.; O'Quinn, B. *Nature* **2001**, *413*, 597.
22. Hsu, K. F.; Loo, S.; Guo, F.; Chen, W.; Dyck, J. S.; Uher, C.; Hogan, T.; Polychroniadis, E. K.; Kanatzidis, M. G. *Science* **2004**, *303*, 818.
23. Flipsen, S. F. J. *J. Pow. Sour.* **2006**, *162*, 927.
24. Dyer, C. K. IEEE – 2004 Symposium On VLSI Circuits Digest of Technical Papers, 2004, 124.
25. Yae, S.; Kobayashi, T.; Abe, M.; Nasu, N.; Fukumuro, N.; Ogawa, S.; Yoshida, N.; Nonomura, S.; Nakato, Y.; Matsuda, H. *Sol. Ener. Mater. Sol. Cells* **2007**, *91*, 224.
26. Mao, S. S.; Chen, X. B. *Int. J. Energ. Res.* **2007**, *31*, 619.
27. Arico, A. S.; Bruce, P.; Scrosati, B.; Tarascon, J. M.; Schalkwijk, W. V. *Nat. Mater.* **2005**, *4*, 366.
28. Maier, J. *Nat. Mater.* **2005**, *4*, 805.
29. Liu, J.; Cao, G. Z.; Yang, Z.; Wang, D.; Dubois, D.; Zhou, X.; Graff, G. L.; Pederson, L. R.; Zhang, J.-G. *Chem. Sus. Chem.* **2008**, *1*, 676.
30. Carlson, D. E.; Wronski, C. R. *Appl. Phys. Lett.* **1976**, *28*, 671.
31. Goetzberger, A.; Hebling, C.; Schock, H. W. *Mater. Sci. Eng. R-Rep.* **2003**, *40*, 1.
32. Goetzberger, A.; Hebling, C. *Sol. Ener. Mater. Sol. Cells* **2000**, *62*, 1.
33. Ward, J. S.; Ramanathan, K.; Hasoon, F. S.; Coutts, T. J.; Keane, J.; Contreras, M. A.; Moriarty, T.; Noufi, R. *Prog. Photovol.* **2002**, *10*, 41.
34. Chopra, K. L.; Paulson, P. D.; Dutta, V. *Prog. Photovol.* **2004**, *12*, 69.
35. Gratzel, M. *Nature* **2001**, *414*, 338.
36. Gratzel, M. *Philos. Trans. R. Soc. London, A* **2007**, *365*, 993.
37. Nelson, J.; Chandler, R. E. *Coor. Chem. Rev.* **2004**, *248*, 1181.
38. Bisquert, J.; Cahen, D.; Hodes, G.; Ruhle, S.; Zaban, A. *J. Phys. Chem. B* **2004**, *108*, 8106.
39. Kroon, J. M.; Bakker, N. J.; Smit, H. J. P.; Liska, P.; Thampi, K. R.; Wang, P.; Zakeeruddin, S. M.; Gratzel, M.; Hinsch, A.; Hore, S.; Wurfel, U.; Sastrawan, R.; Durrant, J. R.; Palomares, E.; Pettersson, H.; Gruszecki, T.; Walter, J.; Skupien, K.; Tulloch, G. E. *Prog. Photovol.* **2007**, *15*, 1.
40. Longo, C.; De Paoli, M. A. *J. Braz. Chem. Soc.* **2003**, *14*, 889.
41. Martinson, A. B. F.; Hamann, T. W.; Pellin, M. J.; Hupp, J. T. *Chem. Eur. J.* **2008**, *14*, 4458.
42. Gratzel, M. *Prog. Photovol.* **2000**, *8*, 171.
43. Oregan, B.; Gratzel, M. *Nature* **1991**, *353*, 737.
44. Nazeeruddin, M. K.; Pechy, P.; Renouard, T.; Zakeeruddin, S. M.; Baker, R. H.; Comte, P.; Liska, P.; Cevey, L.; Costa, E.; Shklover, V.; Spiccia, L.; Deacon, G. B.; Bignozzi, C. A.; Gratzel, M. *J. Am. Chem. Soc.* **2001**, *123*, 1613.
45. Gratzel, M. *J. Photochem. Photobio. C-Photochem. Rev.* **2003**, *4*, 145.
46. Nissfolk, J.; Fredin, K.; Hagfeldt, A.; Boschloo, G. *J. Phys. Chem. B* **2006**, *110*, 17715.
47. Gratzel, M. *Inorg. Chem.* **2005**, *44*, 6841.
48. Gratzel, M. *J. Photochem. Photobio. a-Chem.* **2004**, *164*, 3.
49. Rockstuhl, C.; Lederer, F.; Bittkau, K.; Carius, R. *Appl. Phys. Lett.* **2007**, *91*, 171104.
50. Usami, A. *Chem. Phys. Lett.* **1997**, *277*, 105.
51. Ferber, J.; Luther, J. *Sol. Ener. Mater. Sol. Cells* **1998**, *54*, 265.
52. Rothenberger, G.; Comte, P.; Gratzel, M. *Sol. Ener. Mater. Sol. Cells* **1999**, *58*, 321.
53. Koo, H. J.; Park, J. H.; Yoo, B. J.; Yoo, K. C.; Kim, K. K.; Park, N. G. *Inorg. Chim. Acta,* **2008**, *361*, 677.
54. Anderson, C.; Bard, A. J. *J. Phys. Chem. B* **1997**, *101*, 2611.
55. Barbe, C. J.; Arendse, F.; Comte, P.; Jirousek, M.; Lenzmann, F.; Shklover, V.; Gratzel, M. *J. Am. Cer. Soc.* **1997**, *80*, 3157.

56. Hore, S.; Nitz, P.; Vetter, C.; Prahl, C.; Niggermann, M.; Kern, R. *Chem. Comm.* **2005**, 2011.

57. So, W. W.; Kim, K. J.; Lee, J. K.; Moon, S. J. *Jpn. J. Appl. Phys., Part 1* **2004**, *43*, 1231.

58. Yang, L.; Lin, Y.; Jia, J.; Xiao, X.; Li, X.; Zhou, X. *J. Power Sources* **2008**, *182*, 370.

59. Nishimura, S.; Abrams, N.; Lewis, B. A.; Halaoui, L. I.; Mallouk, T. E.; Benkstein, K. D.; van de Lagemaat, J.; Frank, A. J. *J. Am. Chem. Soc.* **2003**, *125*, 6306.

60. Halaoui, L. I.; Abrams, N. M.; Mallouk, T. E. *J. Phys. Chem. B* **2005**, *109*, 6334.

61. Chou, T. P.; Zhang, Q. F.; Fryxell, G. F.; Cao, G. Z. *Adv. Mater.* **2007**, *19*, 2588.

62. Zhang, Q. F.; Chou, T. P.; Russo, B.; Jenekhe, S. A.; Cao, G. Z. *Angew. Chem. Int. Ed.* **2008**, *47*, 2402.

63. Zhang, Q. F.; Chou, T. P.; Russo, B.; Jenekhe, S. A.; Cao, G. Z. *Adv. Func. Mater.* **2008**. *18*, 1654.

64. Zhang, Q. F.; Dandeneau, C. S.; Zhou, X. Y.; Cao, G. Z. *Adv. Mater.* **2009**, *21*, 4087.

65. Nazeeruddin, M. K.; Kay, A.; Rodicio, I.; Humphrybaker, R.; Muller, E.; Liska, P.; Vlachopoulos, N.; Gratzel, M. *J. Am. Chem. Soc.* **1993**, *115*, 6382.

66. Xu, Y.; Schoonen, M. A. A. *Am. Mineralog.* **2000**, *85*, 543.

67. Chou, T. P.; Zhang, Q. F.; Cao, G. Z. *J. Phys. Chem. C* **2007**, *111*, 18804.

68. Zhang, Q. F.; Dandeneau, C. S.; Candelaria, S.; Liu, D. W.; Garcia, B. B.; Zhou, X. Y.; Jeong, Y. H.; Cao, G. Z. *Chem. Mater.* **2010**, *22*, 2427.

69. Zhang, Q. F.; Dandeneau, C. S.; Park, K.; Liu, D. W.; Zhou, X. Y.; Jeong, Y. H.; Cao, G. Z. *J. Nanophotonics* **2010**, *4*, 041540.

70. Diamant, Y.; Chappel, S.; Chen, S.-G.; Melamed, O.; Zaban, A. *Coor. Chem. Rev.* **2004**, *248*, 1271.

71. Knez, M.; Nielsch, K.; Niinisto, L. *Adv. Mater.* **2007**, *19*, 3425.

72. Rosental, A.; Tarre, A.; Geast, A.; Uustare, T.; Sammelsely, V. *Sens. Actu. B* **2001**, *77*, 297.

73. Aarik, J.; Aidla, A.; Uustare, T.; Ritala, M.; Leskela, M. *Appl. Surf. Sci.* **2000**, *161*, 385.

74. Hamnaa, T. W.; Martinson, A. B. F.; Elam, J. W.; Pellin, M. J.; Hupp, J. T. *J. Phys. Chem. C* **2008**, *112*, 10303.

75. Law, M.; Greene, L. E.; Radenovic, A.; Kuykendall, T.; Liphardt, J.; Yang, P. D. *J. Phys. Chem. B* **2006**, *110*, 22652.

76. Koide, N.; Islam, A.; Chiba, Y.; Han, L. *J. Photochem. Photobio A* **2006**, *182*, 296.

77. Park, K.; Zhang, Q. F.; Garcia, B. B.; Zhou, X. Y.; Jeong, Y. H.; Cao, G. Z. *Adv. Mater.* **2010**, *22*, 2329.